 # 4254R – Revised Version

Quadratite, $AgCdAsS_3$: Chemical composition, crystal structure and OD character

LUCA BINDI,[1,*] PAUL G. SPRY,[2] PAOLA BONAZZI[1], EMIL MAKOVICKY,[3] TONCI BALIĆ-ŽUNIĆ[4]

[1]Dipartimento di Scienze della Terra, Università di Firenze, Via La Pira 4, I-50121 Firenze, Italy
[2] Department of Geological and Atmospheric Sciences, 253 Science I, Iowa State University, Ames, Iowa 50011-3212, U.S.A.
[3]Department of Geography and Geology, University of Copenhagen, Østervoldgade 10, DK-1350 Copenhagen K, Denmark
[4]Natural History Museum of Denmark, Østervoldgade 5-7, D-1350 Copenhagen K, Denmark

ABSTRACT

A re-investigation of the crystal structure of quadratite, ideally $AgCdAsS_3$, was undertaken using a single crystal from the type locality, Lengenbach, Binntal, Switzerland. Average of five electron microprobe analyses led to the empirical formula $(Ag_{0.994}Cd_{0.738}Pb_{0.231}Cu_{0.006}Tl_{0.005}Mn_{0.003}Fe_{0.004}Zn_{0.002}Cr_{0.001})_{\Sigma=1.984}(As_{0.955}Sb_{0.003})_{\Sigma=0.958}S_{3.058}$. Single-crystal structure refinement ($R1$ = 4.84 % for 558 observed reflections) shows that quadratite crystallizes in the space group $P4_322$ and exhibits an atomic arrangement similar to that of the recently approved new mineral manganoquadratite, $AgMnAsS_3$. Like manganoquadratite, quadratite adopts a galena-derivative framework, with metal atoms occupying all the available octahedral interstices, although only M1 and M2 cations, occupied mainly by Cd, adopt a fairly regular octahedral coordination; the M3 cation, occupied by Ag, is located outside the centre cavity in a square-pyramidal coordination, whereas Pb at the split position M3′ coordinates six S atoms. Arsenic also adopts a 3 + 3 asymmetrical coordination, thus forming the AsS_3 pyramidal groups that typically occur in sulfosalts.

The structure can be also described as a stacking of BAB slabs [A: (Cd,Ag)CdS_2 atomic plane; B: (Ag,Pb)AsS_2 atomic plane] along [001]. The rectangular unit cell of these slabs is oriented diagonally to the *a* axes of quadratite and consecutive slabs are related via interlayer two-fold rotation operations parallel either to [100] or to [010]. This ambiguity leads to an OD structure with various possible stacking sequences, from which the tetragonal space group $P4_322$ was observed.

INTRODUCTION

Quadratite, ideally $AgCdAsS_3$, was first found as minute quadratic crystals within cavities of the well known Lengenbach dolomite, Binntal, Switzerland in 1989 and described as a new mineral species only in 1998 (Graeser et al. 1998), when suitable material was found for physical characterization and diffraction data. On the basis of a single-crystal investigation (Weissenberg and precession methods), Graeser et al. determined that the mineral was tetragonal, with a = 5.499(5), c = 33.91(4) Å, space group $I4_1/amd$. An approximate model of the crystal structure of quadratite was then obtained by Berlepsch et al. (1999), by assuming the apparent $I4_1/amd$ crystal symmetry as the result of the superposition of two enantiomorphic structures, having space groups $P4_12_12$ and $P4_32_12$, respectively. According to their model, quadratite can be described as a galena-based derivative framework composed of warped layers parallel to (001) with cations located in distorted octahedral coordinations. Possibly owing to twinning or order-disorder phenomena in quadratite crystals, S atoms are disordered on split positions.

Recently, the new mineral manganoquadratite (Bonazzi et al. 2012) showing a close similarity of formula ($AgMnAsS_3$) and unit-cell dimensions [a_1 = 5.4496(5), c = 32.949(1)] with quadratite has been found in the Uchucchacua polymetallic deposit, Peru. Manganoquadratite crystallizes in the space group $P4_322$ and exhibits a galena-derivative

framework, with S atoms arranged in a cubic closest-packing array with metal atoms occupying all available octahedral interstices. Only the Mn^{2+} cations, however, adopt an octahedral coordination whereas Ag^{+} and As^{3+} are located outside the centre cavities, forming asymmetrical coordination polyhedra, AgS_5 and AsS_3, respectively. In order to substantiate the hypothesis drawn by Bonazzi et al. (2012) and to verify whether or not quadratite is isostructural with manganoquadratite or whether it possesses a different symmetry involving an alternative distribution of the metals within the sulfur close packed structure, a re-investigation of the crystal structure of quadratite was undertaken.

CHEMICAL COMPOSITION

The crystal fragment of quadratite used for the structural study was analyzed with a JEOL JXA-8200 electron microprobe. Major and minor elements were determined at 15 kV accelerating voltage and 30 nA beam current, with 15s as counting time. For the wavelength-dispersion analyses the following lines were used: Ag*L*α, Cu*K*α, Pb*M*α, Cd*K*α, Tl*M*α, Mn*K*α, Fe*K*α, Zn*K*α, Cr*K*α, Sb*L*α, As*L*α, S*K*α. The standards employed were: Ag- pure element (Ag), Cu- pure element (Cu), galena (Pb), Cd- pure element (Cd), synthetic TlTe (Tl), synthetic MnS (Mn), pyrite (Fe, S), synthetic ZnS (Zn), Cr- pure element (Cr), synthetic Sb_2S_3 (Sb) and synthetic GaAs (As). The crystal fragment was found to be homogeneous within the analytical error. The average chemical composition (5 analyses), together with the atomic ratios, is shown in Table 1. On the basis of 6 atoms and on the refinement results, the empirical formula is $(Ag_{0.994}Cd_{0.738}Pb_{0.231}Cu_{0.006}Tl_{0.005}Mn_{0.003}Fe_{0.004}Zn_{0.002}Cr_{0.001})_{\Sigma=1.984}(As_{0.955}Sb_{0.003})_{\Sigma=0.958}S_{3.058}$.

EXPERIMENTAL AND CRYSTAL-STRUCTURE REFINEMENT

A small crystal fragment was selected for the X-ray single-crystal diffraction study from a sample of quadratite from the type locality. Unit-cell parameters, determined by centering

25 high-θ (13-18°) reflections on an automated diffractometer (Bruker MACH3) are given in Table 2. To check the possible presence of diffuse scattering or weak superlattice peaks, the crystal was also mounted (exposure time of 100 s per frame; 40 mA × 45 kV) on a CCD-equipped diffractometer (Oxford Xcalibur™ 3), but no additional reflections were detected. Intensity data were collected using Mo*K*α radiation monochromatized by a flat graphite crystal in ω scan mode. Intensities were corrected for Lorentz-polarization effects and, subsequently, for absorption following the semi-empirical method of North et al. (1968). The values of the equivalent reflections were averaged in the Laue group 4/*mmm*. The merging *R* was 9.72% before absorption correction and decreased to 2.25% for the ψ-scan-corrected data set. E-statistics indicated the structure to be centrosymmetric and the systematic absences gave contradictory information. Nevertheless, given the close similarity of quadratite with the recently approved new mineral manganoquadratite, $AgMnAsS_3$, crystallized in the space group $P4_322$ (Bonazzi et al. 2012), we tried to refine the quadratite structure in the same space group starting with the same set of atom coordinates. The full-matrix least-squares program SHELXL-97 (Sheldrick 2008) was used for the refinement of the structure. The site occupancy of all the metal positions was allowed to vary and, surprisingly, we observed a mean electron number for the Ag position (M3) much greater than 47, suggesting incorporation of a heavier element (i.e. Pb) at this site. Accordingly, Ag was refined vs. Pb with the atomic coordinates of these positions left free to vary independently of each other, while the displacement parameters were constrained to be equal. The refined Pb occupancy for the slightly split M3′ position [M3-M3′ = 0.27(1) Å] was found to be 0.213(4), thus indicating that Pb substitutes for Ag in the quadratite structure, and not for Cd as previously supposed (Graeser et al. 1998). To assign the remaining Ag between the two other metal positions (M1 and M2), their occupancy was tentatively left free to vary (Cd vs. vacancy). The M2 site was found to be fully occupied by Cd, whereas M1 exhibited an electron number

lower than 48, and was then fixed to $Cd_{0.58}Ag_{0.42}$ so as to agree with the chemical formula obtained from the electron microprobe analyses. Finally, the occupancy of the As position was refined versus vacancy but it was found to be fully occupied by arsenic. Neutral scattering curves for Ag, Pb, Cd, As and S were taken from the *International Tables for X-ray Crystallography* (Ibers and Hamilton 1974). Inspection of the difference Fourier map revealed three positive peaks of 4 $e^-/Å^3$ approximately located at about 0.6–0.7 Å from S1, S2 and S3, respectively. However, attempts to introduce these peaks as split sulfur atoms resulted in an unstable refinement and they were disregarded. With anisotropic atomic displacement parameters for all atoms, the *R* value converged to 4.84% for 558 observed reflections [$F_o > 4\sigma(F_o)$] and 60 parameters and at 6.08% for all 1485 independent reflections.

Experimental details and *R* indices are given in Table 2. Fractional atomic coordinates and anisotropic-displacement parameters are shown in Table 3. Table 4[1] lists the observed and calculated structure factors for the quadratite structure.

DISCUSSION

Cation coordination and layer-like configuration

Like manganoquadratite, quadratite possessess a galena-derivative framework, in which a pseudocubic closest-packed array of S atoms has individual (nearly) closest-packed layers stacked along the $[66\bar{1}]$ direction. Metals occupy all the available octahedral interstices, but only M1 and M2 cations adopt a fairly regular octahedral coordination (Table 5); the M3 cation, occupied by Ag, is located outside the centre cavity in a square-pyramidal coordination, whereas Pb at the split position M3′ coordinates six sulfur atoms, with a <Pb-S> mean distance of 2.867 Å (Fig. 1). The AgS_5 square pyramids are quite irregular, with three

[1] For a copy of Table 4, document item AMxxxxx, contact the Business Office of the Mineralogical Society of America (see inside front cover of recent issue) for price information. Deposit items may also be available on the American Mineralogist web site at http://www.minsocam.org.

shorter bond distances at 2.724, 2.747 and 2.78 Å and two longer additional bonds at 2.89 and 2.904 Å, thus adjusting to the trapezoidal environment forced by requirements of As. However, in quadratite Ag is not completely ordered at the M3 site which adopts a (3+2) pyramidal coordination, but also occupies the octahedral M1 site together with Cd. The M2 site, on the other hand, was found to be occupied by Cd only. Like in manganoquadratite, As^{3+} forms typical AsS_3 groups (<As-S> = 2.297 Å).

Alternatively, the structure can be described as a stacking along [001] of square-net planes of S atoms each offset from the adjacent one by ~ ½*a* with respect to the adjacent one. With this arrangement, cations are located inside the mesh of the S_4 square-nets to form two unique planes, $(Cd,Ag)CdS_2$ (A) and $(Ag,Pb)AsS_2$ (B). A-planes are rather regular, whereas the presence of the lone-pair-bearing As^{3+} cation asymmetrically located within the S_4 squared net to bond two sulfur atoms, generates distortion within the square-net plane B. The B-A-B stacking sequence along [001] (Fig. 2) generates slabs of galena-like edge-sharing CdS_6 octahedra, and slabs containing two sets of AgS_5 pyramids whose apices alternatively point upwards and downwards [see Bonazzi et al. (2012) for more details]. It is noted here that galena-like MnS slabs in manganoquadratite correspond to structural modules of alabandite, whereas in quadratite the galena-like CdS slabs do not correspond to any existing mineral. In fact, in both the known CdS polymorphs, hawleyite and greenockite, which exhibit sphalerite and wurtzite structure, respectively, Cd is located in the tetrahedral interstices (<Cd-S> = 2.526 Å, Skinner 1961; 2.532 Å, Xu and Ching 1993). In most sulfides, Cd shows a marked preference for tetrahedral coordination. In the spinel-like structure of cadmoindite, $CdIn_2S_4$, Cd was assumed to be ordered at the tetrahedral site (2.543 Å in the synthetic analogue; Hahn and Klingler 1950); analogously, in the stannite-group minerals černyite, Cu_2CdSnS_4 (Szymański 1978) and barquillite, Cu_2CdGeS_4, (Murciego et al. 1999) Cd enters the tetrahedral sites. However, for (Cd,Pb)-bearing sulfides and sulfosalts like shadlunite,

153 $(Pb,Cd)(Fe,Cu)_8S_8$ (Evstigneeva et al. 1973), kudriavite, $(Cd,Pb)Bi_2S_4$ (Balić-Žunić and
154 Makovicky 2007) and tazieffite, $Pb_{20}Cd_2(As,Bi)_{22}S_{50}Cl_{10}$ (Zelensky et al. 2009), Cd is hosted
155 in octahedral cavities. In particular, in kudriavite an octahedral site was assumed to be mostly
156 occupied by Cd. Its mean bond distance (2.72 Å) and polyhedral volume (26.46 $Å^3$) are in
157 keeping with the corresponding values in the synthetic $CdBi_2S_4$ (2.72 Å and 26.31 $Å^3$; Choe
158 et al. 1997) and perfectly match with the geometrical features of the M2 octahedron in
159 quadratite (Table 5). Bond-valence sums calculated from the curves of Brese and O'Keeffe
160 (1991) are reported in Table 6. The valence units obtained are in perfect agreement with the
161 cation populations assumed in the present study.
162
163 **OD character**
164 Berlepsch et al. (1999) suggested that quadratite has a regular tetragonal net of Cd and S
165 atoms, bordered by layers with trapezoidal configuration and eccentrically positioned cations.
166 Disorder (considerable cation overlapping in the averaged structure) prevented resolution of
167 the structure. Therefore, the most obvious explanation for the assumed disorder was that the B
168 layers can surround the more regular tetragonal A layer in various orientations, resulting in an
169 OD structure.
170 The present investigation, obtained on a (nearly) ordered crystal, however, suggests
171 that the order-disorder phenomena are limited to interspaces between immediately adjacent B
172 layers. If the slight puckering of the B layer is neglected, its plane group symmetry is *cm* with
173 a two-dimensional unit mesh having both dimensions equal to a diagonal of the $a_1 \times a_2$ mesh
174 of quadratite. In the sequence of coordination trapezoids, all short As-S bonds and Ag-
175 displacement point in one direction, diagonal to the crystal axes of quadratite. Rather
176 surprisingly, two B layers surrounding one A layer are oriented parallel to each other and
177 point along the same [110] diagonal but displaced by $\frac{1}{2}[1\bar{1}0]$. This creates linear bonded

groups S2-M2-S2, S3-M1-S3 and M3-S1···As as the only combinations present in the [001] direction of the three-plane B-A-B slab.

This geometrically stable unit is the OD layer of the quadratite structure. If the diagonal in the direction of which the S-As-S configurations point is denoted as the *a* axis of the layer, and the direction perpendicular to the OD layer as the *c* axis (the latter in agreement with the notation of quadratite lattice itself) the layer symmetry symbol will be *C*2*m*(*b*). The glide plane and the two-fold rotation interconnect configurations on the two surfaces of the OD layer. This layer is polar in one intralayer direction and the orientation of the *b*-glide plane perpendicular to the layer-stacking direction is indicated by parentheses.

The most interesting portion of the structure is the interface of two B planes from adjacent OD layers. The sulfur atoms form a trapezoidal net, with a zig-zag trend of S-S distances (3.92-3.96 Å) along the **a** direction of the layer and a straight trend with a regular alternation of shorter (3.39 Å) S-S intervals and longer (4.42 Å) S-S intervals along the **b** direction. As mentioned above, As with its short bonds adheres to the 3.39 Å interval whereas Ag is shifted towards the 4.42 Å S-S interval (Fig. 3). The adjacent B plane is placed in such a way that the pyramidal coordinations of M3 and As of the previous layer are completed to (somewhat distorted) octahedral ones. This places the sulfur atoms of the added B layer approximately above the cations of the preceding layer, with the small deviations balanced as well as possible (Fig. 4). Thus, because of the eccentric position of cations in their planar trapezoidal coordinations, the two sulfur nets are shifted against one another and they are related by two fold rotation axes in the interspace, parallel to *only one* diagonal of the quadratite unit cell (Fig. 4). The zig-zag S-S tie-lines, parallel to the **a** vector of each of the two B planes, are *perpendicular* to one another across the interspace, which is an unique case among sulfosalts.

Trapezoidal schemes of cation-anion planes with zig-zag and straight lines as those observed here are not unusual in sulfosalts (Makovicky and Mumme 1983; Makovicky and Topa 2011). In all these structures, however, orientations of the two atomic planes facing one another are always parallel, with the straight S-S lines running along the infinite direction of the planar configuration, whereas the zig-zag S-S lines are developed along the direction of its limited extent. The unique behavior of the quadratite structure is apparently connected with, in principle, the infinite character of the observed interface. With the orientation of the third short As-S1 bond into the triple B-A-B slab, away from the interface, the interface of two adjacent B planes has a character close to a *lone electron pair micelle* that extends infinitely in two-dimensions.

The interface configuration of atoms described here determines the OD nature of the crystal structure of quadratite (and manganoquadratite, Bonazzi et al. 2012). The two adjacent B planes are either related by a two-fold operation parallel to [100] or, with equal probability, by such an operation parallel to [010] of the quadratite cell, but not both at once. These potential two-fold rotation axes comprise 45^{o} to the **a** and **b** vectors of the layer itself. As the layers are polar, the **a** vector of the generated layer will assume a right-hand or left-hand orientation, always perpendicular to the **a** vector of the initial layer.

What is valid for the B planes is also valid for the entire, polar OD layers. As these layers are non-polar in the layer-stacking direction (contain layer-reversing operations of layer symmetry, so called λ-ρ partial symmetry operators, represented by the *intralayer* two-fold rotation and the *b*-glide; the lambda-rho symbol stands for layer-reversing), the layer-reversing *interlayer* operator (two-fold rotation around [100] of quadratite; it is a so called σ-ρ partial symmetry operator) becomes supplemented by an *n* glide plane parallel to (010) of quadratite (i.e., a layer-nonreversing interlayer operator τ) interspersed between the two-fold rotation axes. The alternative interlayer *n*-glide plane, (100), belongs to the other choice of

227 interlayer partial symmetry elements, namely that which includes 2||[010]. Thus, *n*||(100) and
228 the interlayer rotation [100] mentioned above do not belong to the same choice of symmetry
229 elements and have opposite action, resulting in opposite orientations of the second layer.

230 Tentatively, we can insert the observed elements of OD symmetry into a tetragonal-
231 structured symbol, in agreement with the resulting symmetry of the observed quadratite
232 polytype, with a sequence a_1 a_2 (c) d_1 d_2 in terms of the quadratite lattice [d are the diagonals
233 of tetragonal lattice in the (001) plane]. In this *groupoid symbol* (Dornberger-Schiff 1956), a
234 line with intralayer operators is followed by that with interlayer operators arranged in the
235 same sequence.

236 $$1 \quad 1 \quad (n) \quad 2 \quad m$$

237 $$\{2 \quad n \quad (1) \quad 1 \quad 1\}$$

238

239 There are two structures with the simplest, maximally-ordered stacking sequences, for
240 which all layer pairs are equal (the principal property of OD structures with one kind of layers,
241 as in the present case, distinguishing them from other, less determinate layer-stacking
242 sequences) including layer triples, quadruples, etc.

243 When the same interlayer symmetry element is used (only 2||[100] or only 2||[010]), a
244 polar two-layer sequence results with an *n* glide plane as the universal element. When the
245 active interlayer twofold operations are systematically permutated (e.g., the two fold rotation
246 about a_1, a_2, $-a_1$, $-a_2$, a_1.., connected with the appropriate permutation of symbols in the above
247 two-line *groupoid* symbol), a four-layer structure results, which corresponds to the observed
248 structure $P4_322$ or to its enantiomorph $P4_122$, for which an opposite sequence of axes is used.
249 The λ partial symmetry operations *m* and *b* do not convert into the operations of the space
250 group, only the two-fold intra and interlayer operations do, becoming elements of $P4_322$. Any
251 mistake in this application will result in a non-periodic sequence shift, or in the opposite

enantiomorph or even in non-periodic layer sequences. Mistakes like these were present in the original quadratite material, in which mixing of the $P4_322$ and $P4_122$ structure portions resulted in the *apparent* space group $I4_1/amd$ of a superposition structure, as previously noted by Berlepsch et al. (1999).

ACKNOWLEDGEMENTS

We thank Luca De Battisti who provided us with the quadratite sample from the type locality. This work was funded by "Progetto d'Ateneo 2009" to P. Bonazzi and the research grant no. 09-065749/FNU to E. Makovicky. The manuscript benefited from the revision of S. Mills, R. Peterson, D. Topa, and the Associate Editor D. Gatta.

REFERENCES

Balić-Žunić, T. and Makovicky, E. (2007) The crystal structure of kudriavite, $(Cd,Pb)Bi_2S_4$. Canadian Mineralogist, 45, 437-443.

Berlepsch P., Balić-Žunić, T. and Makovicky, E. (1999) The superposition structure of quadratite $Ag(Cd,Pb)AsS_3$. 1s. Det 30. Danske Krystallografmøde, Forskningscenter Risø, 1999. Abstract 30.

Bonazzi, P., Keutsch, F.N. and Bindi, L. (2012) Manganoquadratite, $AgMnAsS_3$, a new manganese bearing sulfosalt from the Uchucchacua polymetallic deposit, Lima Department, Peru: Description and crystal structure. American Mineralogist, 97, 1199-1205.

Brese, N.E. and O'Keeffe, M. (1991) Bond-valence parameters for solids. Acta Crystallographica, B47, 192-197.

Choe, W., Lee, S., O'Connel, P. and Covey, A. (1997) Synthesis and structure of new Cd-Bi-S homologous series: a study in intergrowth and the control of twinning patterns. Chemistry of Materials, 9, 2025-2030.

Dornberger-Schiff, K. (1956) On the order-disorder structures (OD-structures). Acta Crystallographica, 9, 593-601.

Evstigneeva, T.L., A.D. Genkin, N.V. Troneva, A.A. Filimonova and Tsepin, A.I. (1973) Shadlunite, a new sulfide of copper, iron, lead, manganese and cadmium from copper-nickel ores. Zapiski Vsesoyuznogo Mineralogicheskogo Obshchvestva, 102, 63-74 (in Russian).

Graeser, S., Lustenhouwer, W. and Berlepsch, P. (1998) Quadratite, $Ag(Cd,Pb)(As,Sb)S_3$ – a new sulfide mineral from Lengenbach, Binntal (Switzerland). Schweizer Mineralogische und Petrographische Mitteilungen, 78, 489-494.

Hahn, H. and Klingler, W. (1950) Untersuchungen uber ternare chalkogenide. I. Uber die kristallstruktur einiger ternaerer sulfide, die sich vom In_2S_3 ableiten. Zeitschrift für Anorganische und Allgemeine Chemie, 263, 177-190.

Ibers, J.A. and Hamilton, W.C. Eds. (1974) International Tables for X-ray Crystallography, vol. IV, 366p. Kynock, Dordrecht, The Netherlands.

Makovicky, E. and Mumme, W.G. (1983) The crystal structure of ramdohrite, $Pb_6Sb_{11}Ag_3S_{24}$, and its implications for the andorite group and zinckenite. Neues Jahrbuch für Mineralogie Abhandlungen, 147, 58-79.

Makovicky, E. and Topa, D. (2011) The crystal structure of gustavite, $PbAgBi_3S_6$. Analysis of twinning and polytypism using the OD approach. European Journal of Mineralogy, 23, 537-550.

Murciego, A., Pascua, M.I., Babkine, J., Dusausoy, Y, Medembach, O. and Bernhardt, H-J. (1999) Barquillite, $Cu_2(Cd,Fe)GeS_4$, a new mineral from Barquilla deposit, Salamanca, Spain. European Journal of Mineralogy, 11, 111-117.

North, A.C.T., Phillips, D.C. and Mathews, F.S. (1968) A semiempirical method of absorption correction. Acta Crystallographica, A24, 351-359.

Robinson, K., Gibbs, G.V. and Ribbe, P.H. (1971) Quadratic elongation; a quantitative measure of distortion in coordination polyhedra. Science, 172, 567-570.

Sheldrick, G.M. (2008) A short history of SHELX. Acta Crystallographica, A64, 112-122.

Skinner, B.J. (1961) Unit-cell edges of natural and synthetic sphalerites. American Mineralogist, 46, 1399-1411.

Szymańsky, J.T. (1978) The crystal structure of černyite, Cu_2CdSnS_4, a cadmium analogue of stannite. Canadian Mineralogist, 16, 147-151.

Xu, Y.N. and Ching, W.Y. (1993) Electronic, optical, and structural properties of some wurtzite crystals. Physical Review, B48, 4335-4351.

Zelenski, M., Garavelli, A., Pinto, D., Vurro, F., Moëlo, Y., Bindi, L., Makovicky, E. and Bonaccorsi, E. (2009) Tazieffite $Pb_{20}Cd_2(As,Bi)_{22}S_{50}Cl_{10}$, a new chloro-sulfosalt from Mutnovsky volcano, Kamchatka Peninsula, Russian Federation. American Mineralogist, 94, 1312-1324.

FIGURE CAPTIONS

FIGURE 1- M3 (white) and M3′ (black) sites within the octahedral cavity. Ag at M3 links five sulfur atoms in a square-pyramidal coordination; Pb at M3′ assumes an octahedral coordination. Sulfur atoms are depicted as small gray circles.

FIGURE 2- Succession of (Cd,Ag)CdS_2 (A) and (Ag,Pb)AsS_2 (B) layers stacked along [001]. The B-A-B stacking generates slabs of galena-like edge-sharing CdS_6 and (Cd,Ag)S_6 octahedra (depicted in white), and slabs containing two sets of AgS_5 pyramids (in gray). Arsenic atoms are depicted as black circles.

FIGURE 3- Trapezoidal net of sulfur atoms (B plane) with a zig-zag trend of S-S distances (3.92-3.96 Å) along the $\mathbf{a}_{layer}$ direction and straight trend with a regular alternation of shorter (3.39 Å) S-S intervals and longer (4.42 Å) S-S intervals along the $\mathbf{b}_{layer}$ direction. White, black and gray circles represent Ag at M3, As and S respectively. M3′ site is omitted for clarity. S-S tie-lines are depicted in gray. Long As-S bonds are dashed.

FIGURE 4- Two adjacent B planes shifted against one another and related by two fold rotation axes in the interspace. White, black and gray circles represent Ag at M3, As and S respectively. M3′ site is omitted for clarity. S-S contacts are depicted in gray. Long As-S bonds are dashed. The zig-zag S-S tie-lines, parallel to the **a** vector of each of the two B planes, are perpendicular to one another across the interspace, a case so far unique among sulfosalts.

TABLE 1 – Electron microprobe analyses (means, ranges and standard deviations in wt % of elements) and atomic ratios (on the basis of 6 atoms) for quadratite.

	wt %	range	σ	atomic ratios
Tl	0.23	0.04 – 0.37	0.05	0.005
Ag	26.30	25.42 – 26.63	0.32	0.994
Cu	0.10	0.00 – 0.12	0.03	0.006
Pb	11.72	11.02 – 11.87	0.15	0.231
Cd	20.35	19.79 – 20.68	0.28	0.738
Zn	0.04	0.00 – 0.09	0.01	0.002
Fe	0.06	0.03 – 0.09	0.02	0.004
Mn	0.03	0.01 – 0.06	0.02	0.003
Sb	0.05	0.00 – 0.12	0.02	0.003
As	17.55	16.94 – 18.33	0.23	0.955
Cr	0.01	0.00 – 0.02	0.01	0.001
S	24.04	23.78 – 24.57	0.21	3.058
total	100.48	98.49 – 101.35		6.000

TABLE 2 – Crystallographic data and refinement parameters for quadratite

Crystal data	
Ideal formula	$(Ag,Pb)(Cd,Ag)AsS_3$
Crystal system	tetragonal
Space group	$P4_322$
Unit-cell parameters a, c (Å)	5.5229(4), 33.399(5)
Unit-cell volume (Å^3)	1018.8(2)
Z	8
Crystal size (mm)	0.070×0.090×0.095
Data collection	
Diffractometer	Bruker MACH3
Temperature (K)	298(3)
Radiation, wavelength (Å)	$Mo_{K\alpha}$, 0.71073
θ_{max} for data collection (º)	30.00
h, k, l ranges	0 – 7, 0 – 7, 0 – 46
scan mode, scan width (º), scan speed (°/min)	ω, 2.00, 2.75
Total reflections collected	2324
Unique reflections (R_{int})	1485 (2.25%)
Unique reflections $F > 4\sigma(F)$	558
Absorption correction method	ψ-scan (North et al. 1968)
Structure refinement	
Refinement method	Full-matrix least-squares on F^2
Weighting scheme	$1/\sigma^2(F)$
Data/restraints/parameters	2324/0/61
R_1 [$F > 4\sigma(F)$]	4.84%
R_1 all	6.08%
Largest diff. peak and hole (e$^-$/Å^3)	4.45, -5.00

TABLE 3 – Atoms, site occupancy, fractional atom coordinates (Å), and atomic displacement parameters (Å^2) for quadratite.

atom		site occupancy	*x*	*y*	*z*	U_{iso}	U_{11}	U_{22}	U_{33}	U_{23}	U_{13}	U_{12}
M1	4*c*	$Cd_{0.58}Ag_{0.42}$	0.2429(3)	0.2429(3)	1/8	0.0237(3)	0.0246(4)	0.0246(4)	0.0220(5)	0.0001(4)	-0.0001(4)	0.001(2)
M2	4*c*	$Cd_{1.00}$	0.7382(3)	0.7382(3)	1/8	0.0235(3)	0.0227(4)	0.0227(4)	0.0249(5)	0.0003(4)	-0.0003(4)	-0.001(2)
M3	8*d*	$Ag_{0.787(4)}$	0.748(2)	0.236(2)	0.0337(1)	0.0240(6)	0.0247(8)	0.0286(7)	0.019(1)	0.003(2)	-0.001(2)	-0.0012(9)
M3′	8*d*	$Pb_{0.213(4)}$	0.740(3)	0.242(4)	0.0417(2)	0.0240(6)	0.0247(8)	0.0286(7)	0.019(1)	0.003(2)	-0.001(2)	-0.0012(9)
As	8*d*	$As_{1.00}$	0.2559(3)	0.7443(3)	0.04947(3)	0.0208(2)	0.0206(6)	0.0212(6)	0.0205(4)	0.0001(7)	-0.0007(7)	-0.001(1)
S1	8*d*	$S_{1.00}$	0.2220(7)	0.7364(8)	0.11861(7)	0.0201(6)	0.024(2)	0.018(1)	0.019(1)	0.002(1)	0.003(1)	0.002(2)
S2	8*d*	$S_{1.00}$	0.6646(6)	0.7249(8)	0.0474(1)	0.0254(9)	0.028(2)	0.022(2)	0.026(2)	-0.001(2)	0.004(1)	0.002(2)
S3	8*d*	$S_{1.00}$	0.2334(7)	0.1620(6)	0.04691(8)	0.0208(8)	0.016(2)	0.033(2)	0.014(1)	0.001(1)	0.003(2)	0.002(2)

TABLE 5 – Selected bond distances (Å) for quadratite.

M1	- S3 (x2)	2.647(3)	M2	- S2 (x2)	2.624(3)
	- S1 (x2)	2.736(5)		- S1 (x2)	2.681(4)
	- S1 (x2)	2.808(5)		- S1 (x2)	2.859(4)
mean		2.730	mean		2.721
V_p		26.52	V_p		26.35
σ^2_{oct}		51.5	σ^2_{oct}		43.1
λ_{oct}		1.0161	λ_{oct}		1.0144
M3	- S3	2.724(4)	M3′	- S2	2.71(2)
	- S3	2.747(9)		- S3	2.77(2)
	- S2	2.78(1)		- S3	2.84(2)
	- S2	2.89(1)		- S2	2.89(2)
	- S3	2.904(9)		- S3	2.994(9)
mean		2.810		- S1	2.999(8)
			mean		2.867
As	- S3	2.261(4)			
	- S2	2.312(4)			
	- S1	2.317(3)			
mean		2.297			

Note: the octahedral angle variance (σ^2) and the octahedral quadratic elongation (λ) were calculated according to Robinson et al. (1971); M3-S longer than 3.2 Å are neglected.

TABLE 6 - Bond-valence (*v.u.*) arrangement for quadratite.

	M3	M1	M2	As	Σ S
	$Ag_{0.787}Pb_{0.213}$	$Cd_{0.58}Ag_{0.42}$	Cd	As	
S1		$0.26^{x2\downarrow x1\rightarrow}$, $0.20^{x2\downarrow x1\rightarrow}$	$0.36^{x2\downarrow x1\rightarrow}$, $0.22^{x2\downarrow x1\rightarrow}$,	0.89	1.93
S2	0.23, 0.18		$0.42^{x2\downarrow x1\rightarrow}$	0.90	1.73
S3	0.29, 0.26, 0.16	$0.31^{x2\downarrow x1\rightarrow}$		1.03	2.05
	1.12	1.54	2.00	2.81	

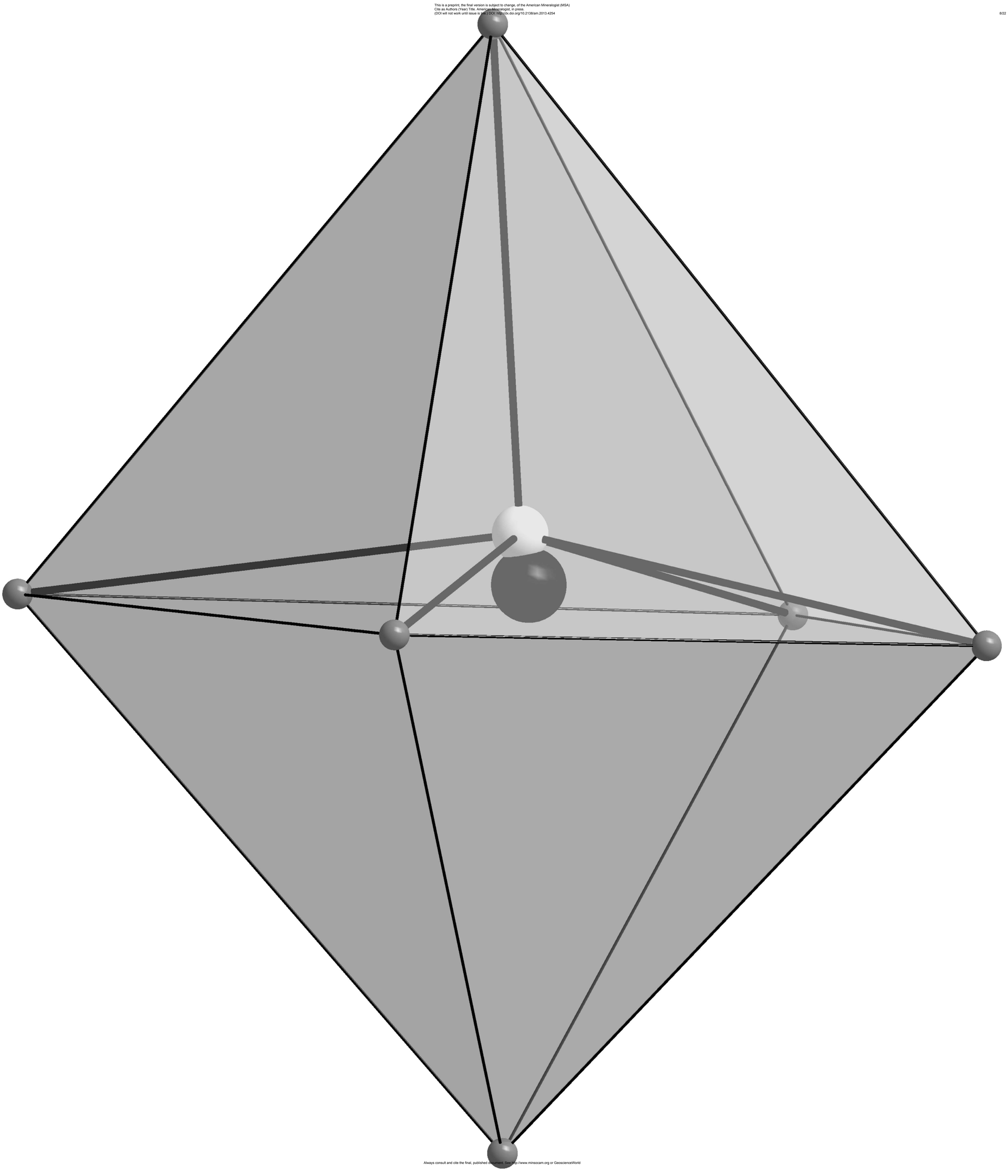

This is a preprint, the final version is subject to change, of the American Mineralogist (MSA)
Cite as Authors (Year) Title. American Mineralogist, in press.
(DOI will not work until issue is live.) DOI: http://dx.doi.org/10.2138/am.2013.4254

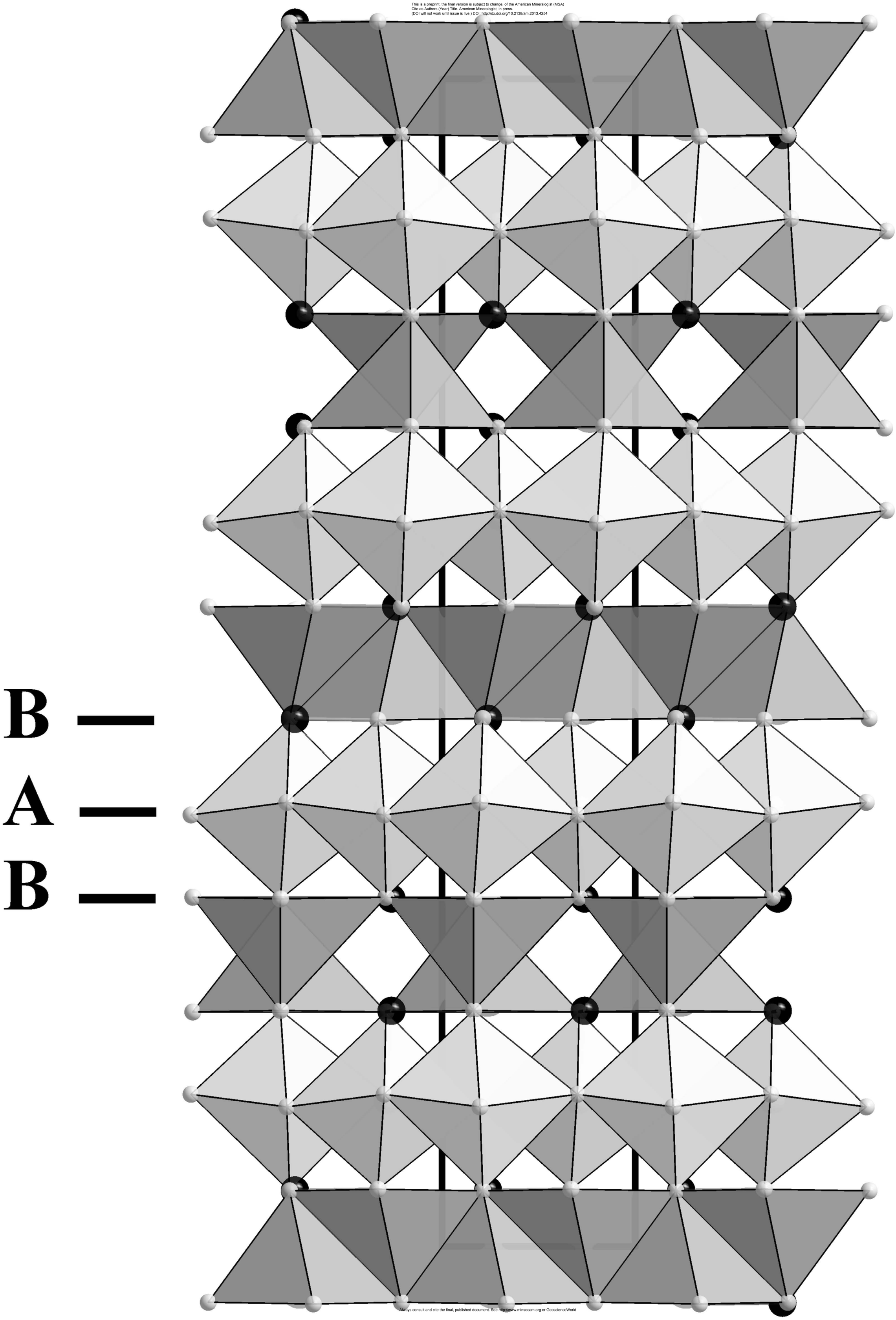

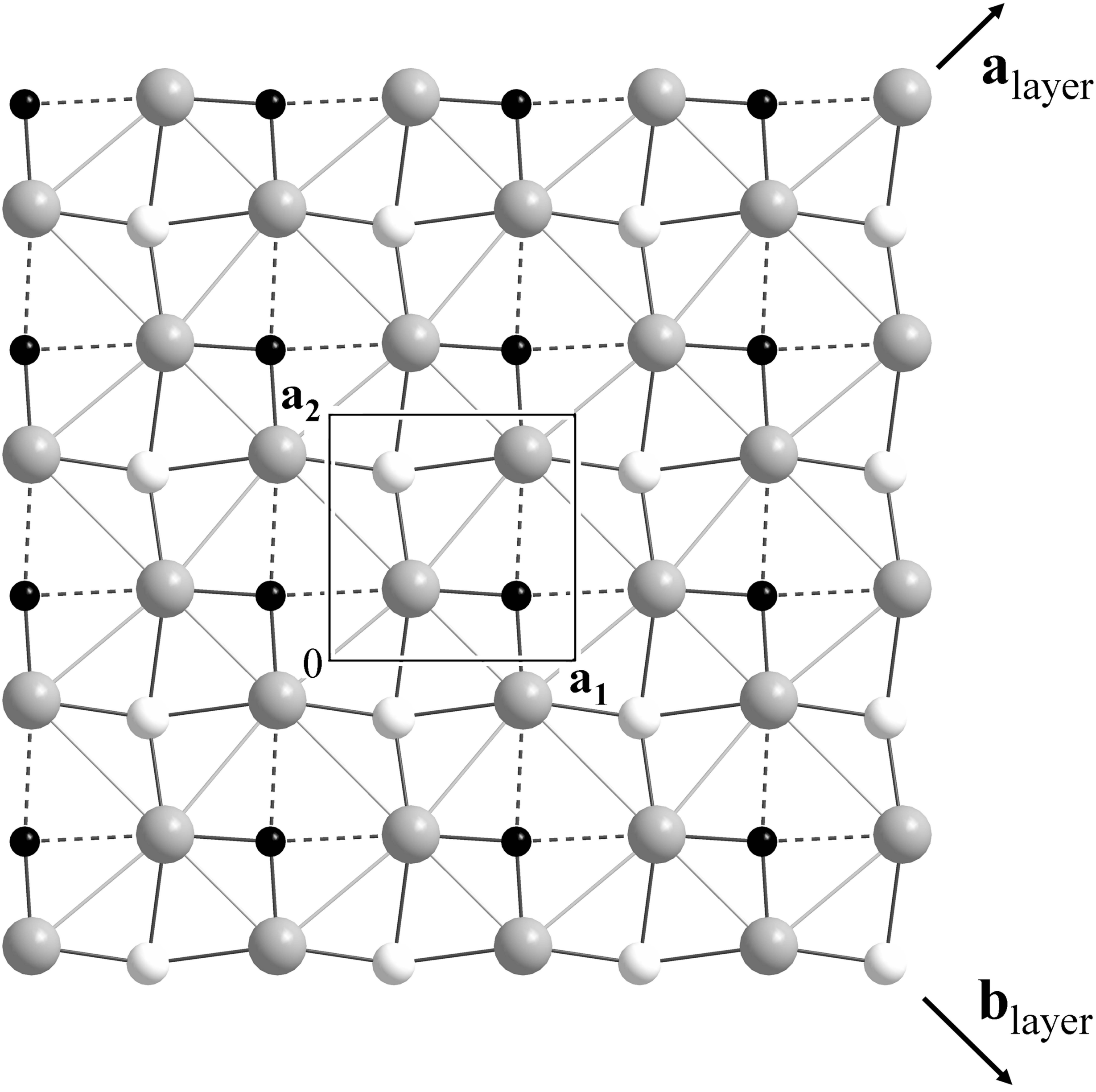

This is a preprint, the final version is subject to change, of the American Mineralogist (MSA)
Cite as Authors (Year) Title. American Mineralogist, in press.
(DOI will not work until issue is live.) DOI: http://dx.doi.org/10.2138/am.2013.4254